Sensors and Actuators B 214 (2015) 181–188

Contents lists available at ScienceDirect

Sensors and Actuators B: Chemical

journal homepage: www.elsevier.com/locate/snb

Resorcinol–formaldehyde aerogels for CMOS-MEMS capacitive humidity sensor

Vincent P.J. Chung [a], Ming-Chuen Yip [a], Weileun Fang [a,b,*]

[a] Power Mechanical Engineering, National Tsing Hua University, Hsinchu, Taiwan
[b] Institute of NanoEngineering and MicroSystems, National Tsing Hua University, Hsinchu, Taiwan

ARTICLE INFO

Article history:
Received 16 December 2014
Received in revised form 9 March 2015
Accepted 13 March 2015
Available online 25 March 2015

Keywords:
CMOS-MEMS
Humidity sensor
Resorcinol–formaldehyde aerogels

ABSTRACT

This paper reports the design, implementation and characterization of a capacitive humidity sensor based on a new kind of organic polymer, resorcinol–formaldehyde (RF) aerogel. The developed fabrication is compatible with CMOS process. In the design, aerogel solution is filled into a vertical parallel-plate (VPP) structure, prepared by the sol–gel method and supercritical fluid (SCF) drying for capacitive sensing. The low-density RF-aerogels synthesized by this method exhibit high surface areas, high porosities, and mesoporosity, which are beneficial to moisture diffusion and sensing reaction. The present sensor shows a sensitivity of 0.595% capacitance change per percent relative humidity (%RH) with a response time of 12 s. Further measurements exhibit maximum hysteresis of 1.1%RH and a 48-h signal drift of 0.75%RH have been obtained. Moreover, temperature calibration of the proposed humidity sensor was carried out. The monolithic integration of an on-chip resistive temperature detector (RTD) with the proposed humidity sensor is thus implemented for the temperature compensated readout.

1. Introduction

Humidity sensors have been widely used in automotive, biomedical, industrial products and domestic appliances. Recently, miniaturized humidity sensors are added into smart phones as personal weather stations and thus have been viewed as one of the most potential emerging sensors in mobile and wearable marketplace. In view of this, the advancement in developing high-performance miniaturized humidity sensors are gaining interests. A number of sensing methodologies have been proposed, including capacitive [1], resistive [2], thermal conductive [3], optical [4], mechanical [5] and resonant [6] types. Due to high sensitivity and linearity over wide humidity range (0–100%RH), less susceptible to temperature changes and low power consumption, the capacitive technique has been extensively investigated [7–11]. Essentially, they can be further categorized into interdigitated electrodes (IDE) [7,9,11] and vertical parallel plate (VPP) [8,10] according to the capacitive structures. Compared with IDE capacitive structures, VPP structures drastically reduce the parasitic signal from air and substrate thus present better sensitivity. However, VPP structures often show an inferior performance in response time due to the much lengthy diffusion path for water vapors.

Using the standard CMOS platforms, miniaturized MEMS devices can be monolithically integrated with electronics. Various CMOS-MEMS capacitive humidity sensors [12–15] have been presented using polyimide sensing films. In [12], four capacitive IDE designs were integrated with an on-chip capacitor-to-current circuit. A maximum sensitivity of 0.9%/%RH was presented. A high aspect ratio IDE design using the stacking of CMOS metal layers was integrated with ring oscillator and heater in [13]. The device with a sensitivity of 25.5 kHz/%RH was operated at 80 °C to avoid signal drifts. A fully packaged capacitive IDE design with integrated heater was reported in [14]. The sensor exhibited a sensitivity of 1.36 fF/%RH. In [15], a capacitive VPP structure with on-chip heater was proposed. The sensor presented a maximum normalized sensitivity of 0.27%/%RH and had claimed to be at least 17% more sensitive than the most IDE design integrated with CMOS.

As for the moisture sensitive films, polymer-based and especially polyimide-based sensors have been extensively used inasmuch as the superior properties over wide humidity range and the compatibility with CMOS platforms. However, polyimides feature slow diffusion constant [7,15] and relatively high curing temperature (300 °C) [7,12] with regard to the reliability of metal layers and performance of transistors in the CMOS standard process. The porous materials such as anodic aluminum oxide [16], porous silicon [17], mesoporous silica [18] and silica aerogel

* Corresponding author at: Power Mechanical Engineering, National Tsing Hua University, Hsinchu, Taiwan. Tel.: +886 3 574 2923; fax: +886 3 5739372.
E-mail address: fang@pme.nthu.edu.tw (W. Fang).

http://dx.doi.org/10.1016/j.snb.2015.03.024
0925-4005/

[19,20] for the application of humidity sensors were also reported. These materials provide high contact areas to water molecules and enable free molecules to past through the pores with relative ease. Inasmuch, porous materials are potential for the enhancement of sensitivity and response time of a humidity sensor. Silica aerogel, a mesoporous material with cross-linked nanostructure and high porosity, shown great potential in humidity sensing was reported in [19]. Silica-aerogel thin films were screen printed on IDE for electrical testing at different humidity levels. The electrical sensing properties, in particular, impedance of silica aerogels to humidity were extensively investigated in [20]. The test results indicated the potential capability of silica aerogels for humidity sensing. However, the preparation process of silica aerogels is well above 500 °C and thus not suitable for the standard CMOS process.

In general, this paper presents a capacitive humidity sensor using the CMOS-MEMS technique. A new kind of aerogel–RF-aerogel was introduced in this work. The RF-aerogel offers the advantages of both porous materials as well as polymers. Also, the capability to integrate with CMOS platforms was further proven. By extending the concept in [21], the proposed design has integrated mesoporous RF-aerogels into a VPP structure as the moisture sensitive film. Thus, a submicron gap VPP with an improvement on sensor response time is designed and implemented. The performance measurement has been carried out over a humidity range of 15–95%RH at 30 °C. Moreover, the evaluation of hysteresis, stability and response time has been performed. The temperature calibration of the proposed humidity device under a typical operating range of 20–50 °C was characterized. To consider the influence of temperature on readout signal, the monolithic integration of a resistive-type temperature sensor with the humidity sensor is thus implemented.

2. Concept and design

Fig. 1 presents the schematics of the proposed relative humidity (RH) sensor design. The commercial available standard TSMC (Taiwan Semiconductor Manufacturing Co.) 0.18 μm 1P6M (1-polysilicon and 6-metal layers) CMOS process is employed to implement the presented device. Note the six metal layers are respectively denoted as M1 (metal-1 layer) ~M6 (metal-6 layer) in this study. Thus, the design rules for this standard CMOS process has to be followed. As shown in Fig. 1(a), the design of proposed humidity device consists of a circular VPP capacitor (diameter D = 475 μm) with equally spaced etch/vent holes and oxide pillars. In addition, the schematic cross-section view along the AA′ is further shown in Fig. 1(b). The aerogel is filled between the two circular sensing plates. The effective dielectric constant of aerogel varies with the amount of absorbed water vapor and thus induces changes in capacitance of VPP capacitor under different RH levels. Note that a dispensing target was utilized to allow aerogel solution to flow through the dispensed channel and further fill into the submicron gap between the two vertical sensing plates.

Fig. 1(c) further shows the detailed structure design, layers stacking, and dimensions, of the sensor. The sectioning view of the sensor as marked with BB' is also presented. The M2 and M4 metal layers are respectively acted as the bottom and top sensing electrodes. Moreover, the M3 metal film is used as the sacrificial layer. After removing the M3 layer by metal wet etching, the submicron sensing gap of 0.53 μm is defined by the film thickness. The circular VPP capacitor is anchored on the edge of the sensing plates. In addition, 53 oxide pillars were also added to support the top plate of a VPP so as to ensure sensors integrity and the process yield. In summary, with the design of oxide pillar, this study enables the implementation of large area VPP with submicron sensing gap to enhance the sensitivity of the proposed humidity sensors. For the proposed large area VPP design, the periodic holes on sensing plate are designed not only to act as release holes for the metal wet etch but also to provide access path for water vapor to the aerogel layer. Thus, the response time of the sensor can be improved. Note that the sensing area will be decreased with the existing of etch/vent holes. In this design, the area of vent holes is near 20% of the footprint of VPP plate ($\pi D^2/4$). In other words, the fill-factor of the sensing electrode on the VPP plate is 80%. The sensitivity and response time of the sensor can be further modulated by varying the area of vent holes.

Most of the existing VPP electrodes were designed and fabricated in direct contact with moisture sensitive dielectrics. Such design could lead to a relatively low break down voltage as the dielectrics thin down to submicron level [8]. In addition, long-term exposure of VPP electrode to high humidity levels also poses a serious concern for its reliability [11], and a possible short circuit of the capacitance stemmed from the condensation of water between sensing electrodes. Accordingly, this study takes the advantage of CMOS processes to employ the existing dielectric oxide layers to protect the metal sensing electrodes. Nonetheless, the dioxide cover is intrinsically inert to water vapor, thereby degrading the sensitivity of the device.

The preparation processes of RF-aerogels, in this work, are based on the reported sol–gel methods [22,23]. Supercritical carbon dioxide (CO_2) drying is included to avoid shrinkage of the solid matrix. The RF-aerogels prepared by these methods, exhibit high porosity (>80%), high surface areas (400–900 $m^2\,g^{-1}$), and low densities (0.03–0.079 $g\,cm^{-3}$). In comparison, RF-aerogels exhibit higher diffusion constant than polyimides and the preparation processes could be held at room temperature. In addition, owing to the hydroxyl groups, RF-aerogels show hygroscopic nature. Upon water absorption, properties of RF-aerogels such as higher surface area along with the lower dielectric constant (ε = 2–3) could provide better capacitance changes than polyimides, since water is a polar molecule with a dielectric constant of 80 [7].

3. Fabrication and results

The fabrication process for the humidity sensor is shown in Fig. 2. Beginning with a standard CMOS chip fabricated by TSMC 0.18 μm 1P6M CMOS process (Fig. 2(a)), a metal wet etch process [24] is performed to release the VPP structure to form a vertical gap (Fig. 2(b)). The VPP structure was released by deploying M3 layer in the CMOS stack as sacrificial layers to create a 0.53 μm vertical gap that can be filled subsequently with RF-aerogels. The electrodes of the VPP capacitor thus formed are comprised of M2 and M4 layers with dielectric coverage. The dielectric layers, silicon dioxide, serve as the protective coverage of the electrodes during the wet etching and isolation from chemicals after the device was fabricated. In other words, through metal wet etch process, Al electrodes of the VPP capacitor are covered with dielectric layers to ensure the reliability of sensors. An anisotropic reactive-ion etching was then used to remove the passivation for pad opening (Fig. 2(c)). Afterwards, resorcinol–formaldehyde solution was directly dispensed into the target, filled fully between the vertical gap (Fig. 2(d)). Resorcinol and formaldehyde solution was mixed at a volume ratio of 1:1. The dispensed volume of RF solution was well-controlled by the dispensing time and pressure of a commercial pneumatic dispensing workstation (EFD 2400, EFD Inc.). Through poly-condensation of resorcinol with formaldehyde in the presence of sodium carbonate (Na_2CO_3) as a base catalyst, the RF solution (resorcinol/catalyst ratio of 100) was cured in a hermetically sealed container in room temperature. The resulting solid wet gel was then washed with acetone for solvents exchange. To avoid collapse or shrinkage of the structure, as the solvent-containing

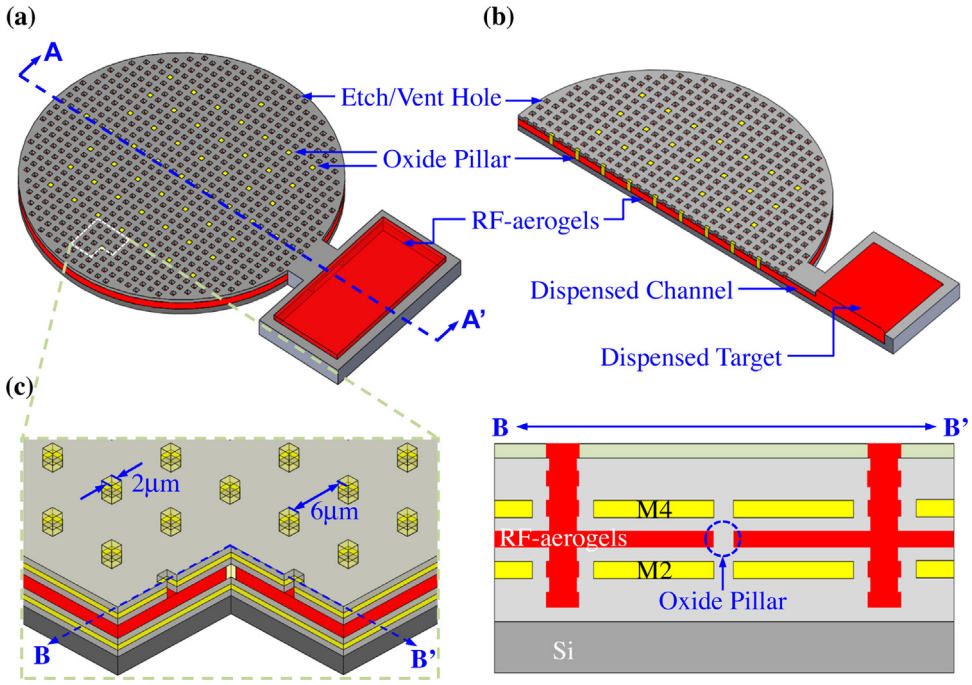

Fig. 1. Illustration of the design concept: (a) the proposed CMOS-MEMS humidity sensor with RF-aerogels filling, (b) cross-section view and (b) magnified view of the detailed design.

gel is formed, a CO_2 SCF drying process was then carried out (30 °C, 14 MPa) to obtain an open-cell nanostructure with high porosity. Note that the deposition processes of RF-aerogels were all kept at low temperatures. In comparison, polyimide-based devices were also fabricated through the aforementioned process steps except that polyimides were dispensed into the target as shown in Fig. 2(d). The polyimide (Durimide 100, Fujifilm) was thermal cured at a cycle up to 350 °C. Note the maskless post-CMOS processes are achieved in Fig. 2(b)–(d).

Micrographs in Fig. 3 respectively show the fabricated devices filled with RF-aerogels and polyimides. As shown in Fig. 3(a), an undispensed humidity device and an integrated temperature sensor are displayed. The temperature sensor is a resistive-type temperature sensor. Where, a serpentine polysilicon trace was deployed and served as the resistive temperature detector (RTD). Fig. 3(b) further shows the zoom-in view of the etch/vent holes after the deposition of RF-aerogels. Scanning electron micrographs (SEM) in Fig. 3(c) and (d) show the fabricated humidity sensors with RF-aerogels and polyimides filling, respectively. Both sensors were characterized through the following performance tests to evaluate the prospective potential of RF-aerogels. By inspection of SEM, the proposed design of dispensed targets and channels allows polymers to fill the VPP gap perfectly without discovery of unfilled holes and residuals from the overflow of RF solution. Fig. 3(e) further shows the focused ion beam sectioning of the presented device after the deposition of RF-aerogels. The VPP structure was released

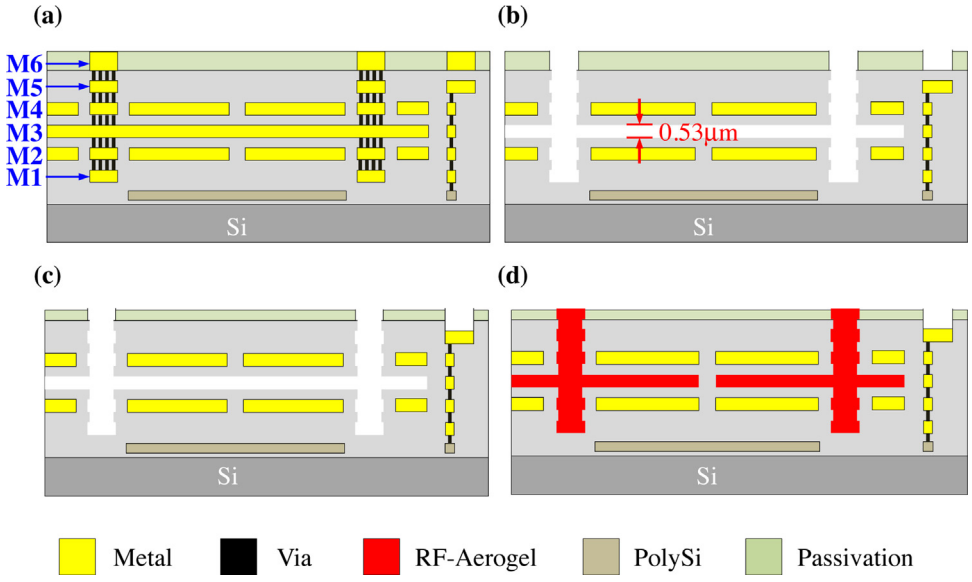

Fig. 2. Schematic drawings of the main CMOS-MEMS post-processing steps: (a) TSMC 0.18 μm 1P6M CMOS chip, (b) metal wet etch, (c) RIE passivation etch, and (d) deposition of RF-aerogels.

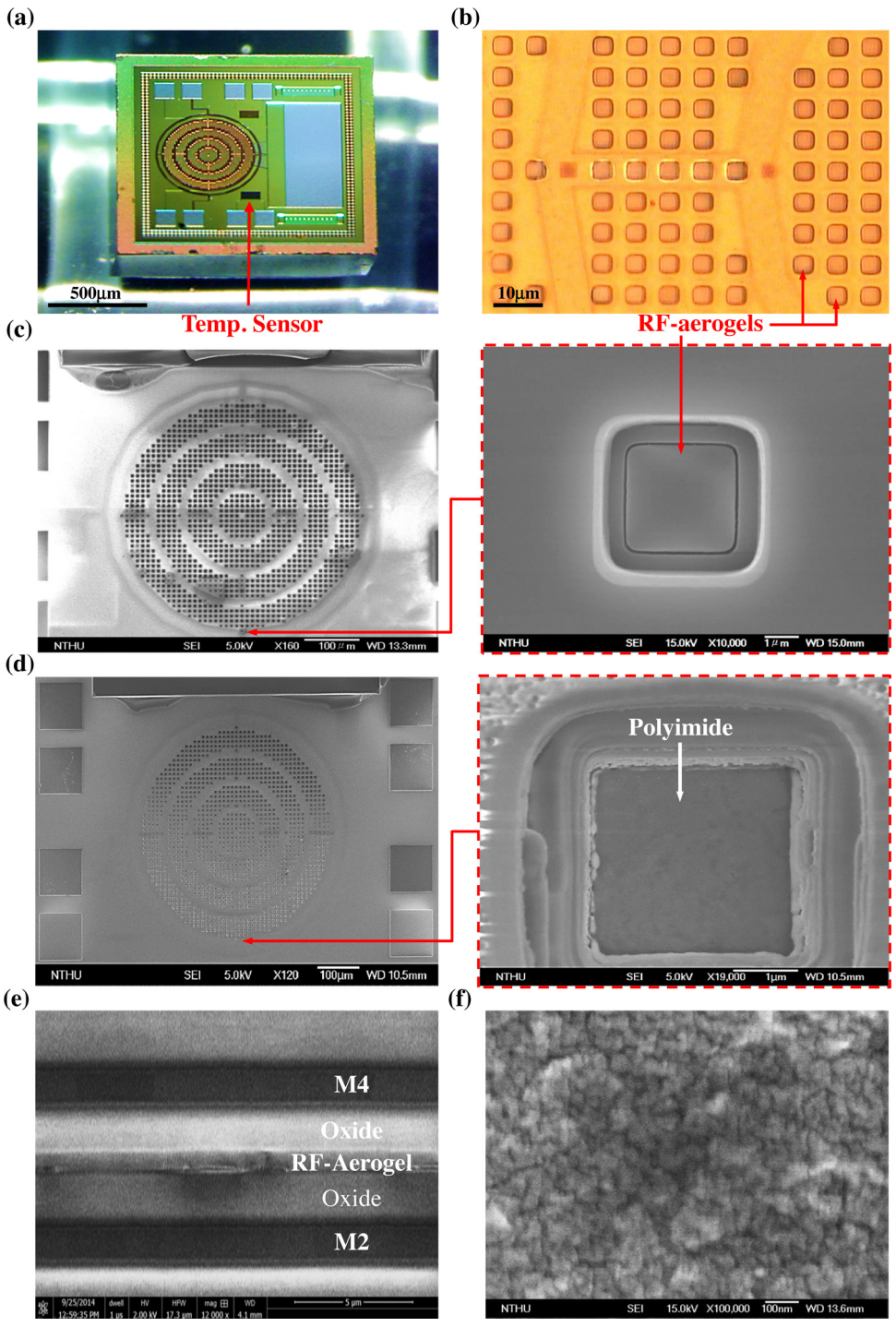

Fig. 3. Optical images of the fabrication results (a) before, and (b) after the deposition of the RF-aerogels. Scanning electron micrographs (SEM) showing the fabricated sensors: top view of the (c) RF-aerogel and (d) polyimide sensor with detailed images of the vent holes furthest from the dispensing channels. (d) FIB cross section with 0.53 μm RF-aerogel fill-in gap. (g) Nanostructures of the deposited RF-aerogels.

successfully with a submicron gap of 0.53 μm and RF-aerogels filled fully into the gap without notable flaws. As shown in Fig. 3(f), the SEM examination shows the morphology of mesoporous RF-aerogels.

4. Experiments and discussions

This study performed various tests to demonstrate the performances of the presented humidity sensor. Firstly, the surface profile of the proposed RF-aerogel-based sensor was verified and displayed through a commercial optical interferometer. The maximum deflection of the fabricated device along the CC′ cross section in Fig. 4 is less than 0.25 μm. The measurement set-up in Fig. 5 was established to characterize the capacitance changes of fabricated devices at different humidity controlled by chamber. The device under test (DUT) was bonded to a printed circuit board and put inside a sealed chamber for sensor characterization. Meanwhile, the DUT mounted on a printed circuit board (PCB) was wire-connected to the LCR meter (Agilent E4980A). The capacitance values at different humidity were recorded by a computer. Note that a commercial

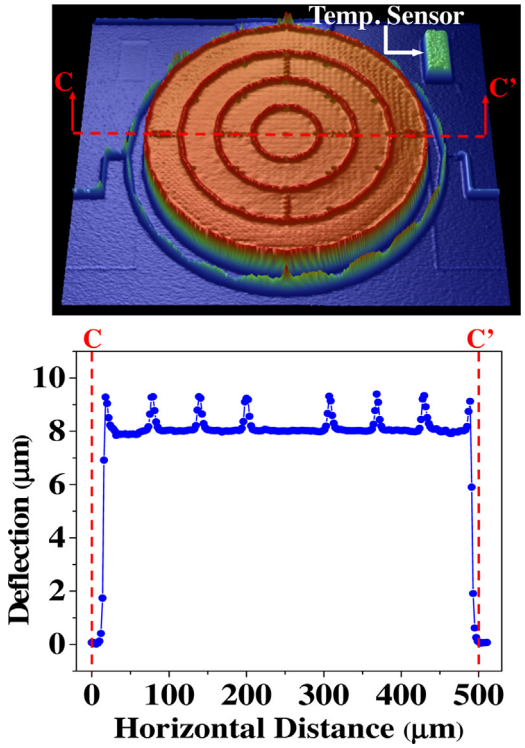

Fig. 4. Optical interferometer surface measurement of the fabricated sensor with RF-aerogel filling.

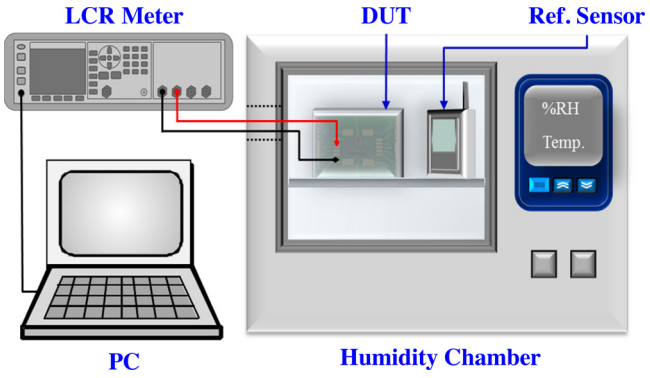

Fig. 5. Schematic diagram of the measurement setup for capacitive relative humidity (RH) sensors.

humidity/temperature sensor (Sensirion SHT21) was used as a reference to monitor the precise temperature and RH level inside the chamber. By placing the chip on a temperature controlled stage (Linkam Ltd., THMS600), the resistance change of RTD was then characterized and recorded by a source meter (2700, Keithley Instruments Inc.) at different temperatures with intervals of 5 °C. Note that the resistance of RTD was recorded as it reached a stable value. Such measurements could show the variation of RTD resistance with the temperature. The characterizations of the proposed sensors are presented as follow.

4.1. Sensitivity

Firstly, the sensitivity of presented humidity sensor with RF-aerogels filling was characterized. The humidity sensor with polyimide filling was also characterized as a reference for sensing performances. Measurements have been taken at 30 °C, humidity levels within the range of 15–95%RH and the LCR meter at a

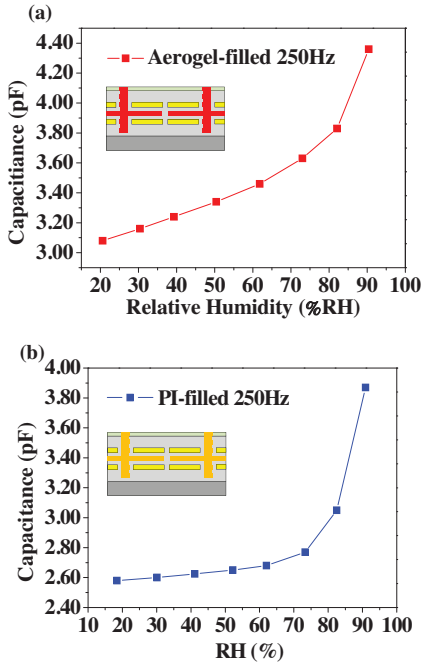

Fig. 6. Sensitivity measurement of the fabricated sensors with (a) polyimide filling and (b) RF-aerogel filling. The measurement was conducted at 30 °C and the operating frequency of 250 Hz.

driving frequency of 250 Hz. The typical capacitance output of sensors is shown in Fig. 6 as a function of relative humidity with measuring intervals of 10%RH. The normalized sensitivity Sn (defined as the percentage change of capacitance per percent RH, i.e. %/%RH) is employed to evaluate the performance of the humidity sensors. For humidity sensors of identical topology design, their normalized sensitivity is totally contributed by the dielectric change of sensing material upon water absorption. As depicted in Fig. 6(a), the normalized sensitivity Sn (at the sensing range of 18–83%RH) of the RF-aerogel-based humidity sensor is 0.595%/%RH. As shown in Fig. 6(b), the normalized sensitivity Sn (also at the sensing range of 18–83%RH) of the polyimide-based humidity sensor is 0.284%/%RH. As comparison with the polyimide-based humidity sensor, the RF-aerogel-based one presents a two-fold sensitivity enhancement. Since the humidity sensors for Fig. 6(a) and (b) have the identical VPP structure, the measurements indicate that RF-aerogel is much more sensitive to water vapor than polyimide. Moreover, other reported polyimide-based sensors are listed in Table 1 for comparison. Due to water condensation on the device, it is noted that both measurements in Fig. 6 exhibit an escalation of capacitance as relative humidity above 90%. Typically, this issue could be solved by heating up the humidity sensor [13,14], thereby reducing the ambient RH that a sensor exposed to.

4.2. Hysteresis and stability

The moisture sensitive film of a humidity sensor will be influenced by its exposure history [25]. The resulting hysteresis effect could adversely affect the accuracy of a sensor and thus have been set as an important parameter to be further evaluated. Herein, measurements have also been performed at 30 °C to investigate the hysteresis behavior of the proposed humidity sensor under an absorption–desorption cycle as shown in Fig. 7. The maximum measurement uncertainty due to the hysteresis effect is 0.61%RH at 51.9%RH, which is less than a general rule of thumb of 1%RH. Moreover, as exposed to high humidity ambient, the output of a

Table 1
Performance comparison of several published capacitive humidity sensors.

	Kang [7]	Boltshauser [12]	Dai [13]
Process	Si-based	CMOS-based	CMOS-based
Sensitive film	Polyimide	Polyimide	Polyimide
Foot print	$1000 \times 1300\ \mu m^2$	$380 \times 380\ \mu m^2$	$1000 \times 1000\ \mu m^2$
Sensitivity	0.38%/%RH	0.9%/%RH	25.5 kHz/%RH
Response time	1 s (ΔRH: 57%)	<30 s (ΔRH: 15%)	N/A
Hysteresis	N/A	<1% RH	N/A
Drift (48 h)	N/A	<4% RH	N/A
	Lazarus [15]	**Chung [21]**	**This study**
Process	CMOS-based	CMOS-based	CMOS-based
Sensitive film	Polyimide	RF-aerogel	RF-aerogel
Foot print	$150^2 \times \pi\ \mu m^2$	$475 \times 475\ \mu m^2$	$240^2 \times \pi\ \mu m^2$
Sensitivity	0.27%/%RH	0.571%/%RH	0.595%/%RH
Response time	70 s (ΔRH: 3%)	19 s (ΔRH: 60%)	12 s (ΔRH: 60%)
Hysteresis	N/A	1.1% RH	0.61% RH
Drift (48 h)	N/A	0.75% RH	0.94% RH

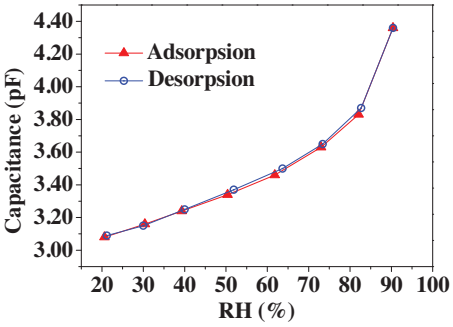

Fig. 7. A hysteresis measurement of the proposed sensor under an absorption–desorption cycle at 30 °C.

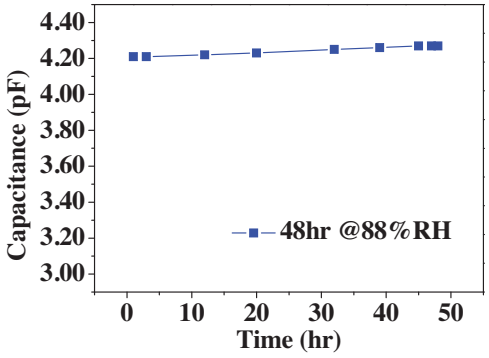

Fig. 8. Stability test of the sensor at 30 °C and 88%RH for 48 h.

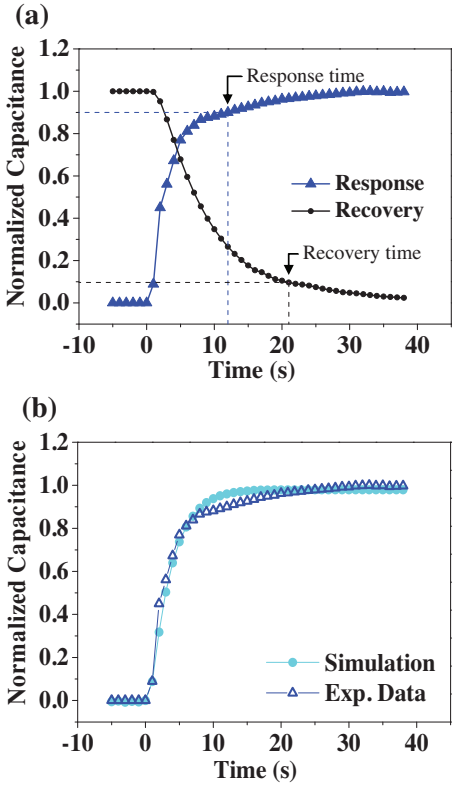

Fig. 9. Measured response and recovery time of (a) the proposed sensor with step changes from 20%RH to 80%RH and the reverse at 30 °C, and (b) evaluation of the corresponding diffusion constant using COMSOL simulation.

capacitive humidity sensor will gradually undergo an upward signal drift [7,12]. In general, the amount of drift is proportional to the magnitude of RH and the length of exposure. In this study, a 48-h stability test under 88%RH condition was performed at 30 °C. Measurements in Fig. 8 depict the output characteristic of the proposed sensor over 48 h. The sensor exhibits a relatively low drift of 0.06 pF (0.94%RH) in maximum and compares favorably with existing sensors.

4.3. Response time

As shown in Fig. 9, a step change from 20%RH to 80%RH was conducted at 30 °C so as to determine the response time of sensor. In this study, the response time is defined as the time for a sensor to reach 90% of the final capacitance value [7,12]. As shown in Fig. 9(a) the response time of the proposed humidity sensor is 12 s (as indicated by the dash line, the normalized capacitance increased from 0 to 0.9). As shown in Fig. 9(a), recovery process of the sensor from 80%RH to 20%RH was carried out likewise. The recovery time is 21 s (as indicated by the dash line, the normalized capacitance decreased from 1.0 to 0.1) which takes slightly longer than the response time. This is mainly due to the difficulty in desorbing the chemisorbed water molecules on the accessible hydroxyl sites on the surface of RF-aerogels at low humidity level [26]. A possible solution to expedite the recovery process is to incorporate an embedded polysilicon heater in CMOS process [15].

Through the experimental data, the diffusion constant of water vapor into RF-aerogels can be estimated by finite element analysis. Fig. 9(b) further shows the step change curves (from 20%RH to 80%RH) determined from measurement and COMSOL simulation.

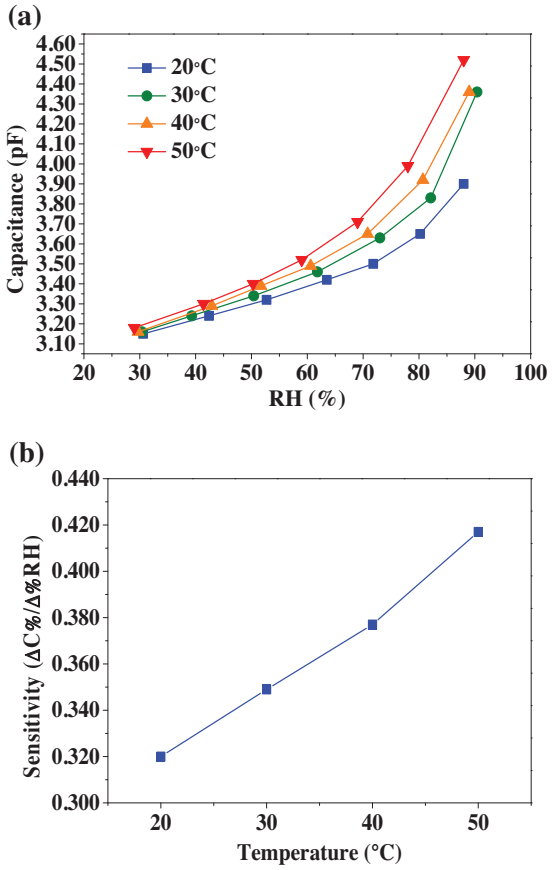

Fig. 10. Sensitivity measurement results of: (a) the characteristic curves at 20–50 °C and (b) sensitivity as a function of temperature.

It indicates the COMSOL simulation agrees well with the measurements as the diffusion constant of RF-aerogels is specified as 5×10^{-11} m^2/s. Thus the diffusion constant of RF-aerogels is determined, and then the response time of other designed topologies using RF-aerogels can be predicted. In comparison, the diffusion constant of RF-aerogel is at least one order higher than that of the polyimide (1.5×10^{-13} m^2/s) reported in [15]. Theoretically, the response time of the humidity sensor is comparatively faster with the filling of RF-aerogel than polyimide under an identical capacitive sensor topology.

4.4. Temperature calibration

Measurements in Fig. 10(a) indicate the capacitance changes of the present humidity sensor as relative humidity varying from 30%RH to 90%RH. The measurements were performed under different ambient temperatures (ranging from 20 °C to 50 °C). The sensitivity S (defined as the capacitance change per percent RH, i.e. ΔC/%RH) of the humidity sensors is used for the following discussion. At low humidity levels (<30%RH), the initial capacitance is almost invariable with temperature and thus each characteristic curve approaches to a fixed constant. In addition, the sensitivity of sensor is increased with the increment of temperature. Fig. 10(b) further shows the sensitivity S of humidity sensor (determined from the measurements in Fig. 10(b) within the relative humidity range of 29–88%RH) versus temperature. The calibration of sensitivity S shows a linear relation with temperature. The fitted equation of the data can be expressed as:

$$S = 1.04 \times 10^{-4} T + 7.93 \times 10^{-3} \quad (1)$$

where T (°C) is the ambient temperature.

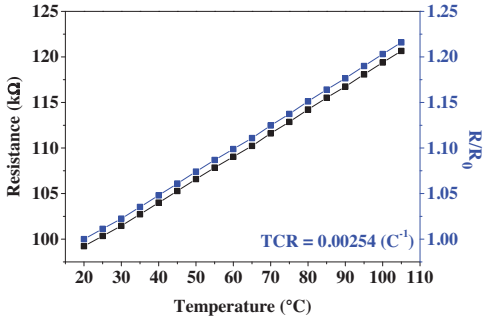

Fig. 11. Temperature calibration of the on-chip polysilicon RTD. A temperature coefficient of resistance (TCR) of 0.00254 °C^{-1} was measured.

Since the temperature sensitivity cannot be ignored, the RTD shown in Fig. 3(a) is monolithically integrated with the humidity sensor on the CMOS chip. The equation corresponding to the temperature calibration of the proposed humidity sensor was presented. Measurements in Fig. 11 indicate that the resistivity of the polysilicon increases linearly with the temperature over the range from 20 °C to 105 °C. After the liner fit of results in Fig. 11, the temperature determined from the measured resistance of RTD can expressed as:

$$T = 3.909 \times R - 366.454 \quad (2)$$

where R (kΩ) is the resistance of RTD. In addition, the temperature coefficient of resistance (TCR) of the RTD sensor is 0.00254 °C^{-1}. By the substitution of Eq. (2) into Eq. (1), signal drifts of the humidity sensor due to temperature variation is given by:

$$\Delta\%\mathrm{RH} = \frac{\Delta C}{(4.06 \times 10^{-4})R - (3.02 \times 10^{-3})} \quad (3)$$

Through the integration of the on-chip RTD, Eq. (3) provides a temperature compensation for the proposed humidity sensor. Therefore, a precise humidity value can be given at different temperatures. Fig. 12 further displays a three-dimensional plot based on Eq. (3). Thus, the relative humidity could be determined from the ΔC and R respectively measured from the proposed humidity and RTD sensors.

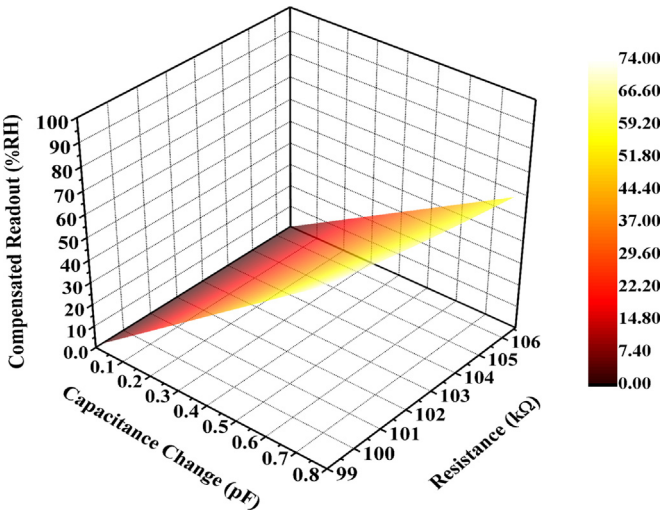

Fig. 12. A three-dimensional diagram of the proposed temperature compensation for the presented humidity sensor.

5. Conclusions

This study presents the design, fabrication, and characterization of a VPP capacitive humidity sensor based on the CMOS processes and RF-aerogel material. The proposed sensor was successfully implemented using the TSMC 0.18 μm 1P6M CMOS standard process along with the in-house post-processing of the CMOS chip. Along the fabrication process, the filling conditions as well as the morphology of RF-aerogels were inspected and proven through SEM. The sensor was measured to have the sensitivity in a capacitance change of 0.595% per percent RH, which presented a two-fold increase over the polyimide-based sensor in sensitivity. Additionally, the proposed high fill-factor (80%) design showed a response time of 12 s. A maximum hysteresis of 0.61%RH at 51.9%RH has been obtained. At 88%RH for 48 h, the sensor exhibited a signal drift of 0.94%RH. To provide an accurate compensation for humidity sensing, temperature calibration of the humidity sensor through an on-chip temperature sensor was proposed. Table 1 summarizes the typical measured performances of the present humidity sensor in comparison with other polymer based capacitive sensors. In summary, the RF-aerogel is a promising material for the application of humidity sensor.

Acknowledgements

The authors would like to thank the TSMC and the National Chip Implementation Center, Taiwan, for the support of CMOS chip manufacturing. The authors would also like to appreciate the Central Regional MEMS Research Center of National Science Council, and the National Nano Device Laboratory of NSC for providing the fabrication facilities.

References

[1] N. Lazarus, S.S. Bedair, C.C. Lo, G.K. Fedder, CMOS-MEMS capacitive humidity sensor, J. Micromech. Microeng. 19 (2010) 183–191.
[2] Q.-Y. Tang, Y.C. Chan, K. Zhang, Fast response resistive humidity sensitivity of polyimide/multiwall carbon nanotube composite films, Sens. Actuators B 152 (2011) 99–106.
[3] B. Okcan, T. Akin, A thermal conductivity based humidity sensor in a standard CMOS process, in: Proc. 17th IEEE Int. Conf. Micro Electro Mechanical Systems (MEMS), Maastricht, Netherlands, 25–29 January, 2004, pp. 552–555.
[4] Y.J. Liu, J. Shi, F. Zhang, H. Liang, J. Xu, A. Lakhtakia, et al., High-speed optical humidity sensors based on chiral sculptured thin films, Sens. Actuators B 156 (2011) 593–598.
[5] C.-Y. Lee, G.-B. Lee, Micromachine-based humidity sensors with integrated temperature sensors for signal drift compensation, J. Micromech. Microeng. 13 (2003) 620–627.
[6] H.-S. Hong, D.-T. Phan, G.-S. Chung, High-sensitivity humidity sensors with ZnO nanorods based two-port surface acoustic wave delay line, Sens. Actuators B 172 (2012) 1283–1287.
[7] U. Kang, K.D. Wise, A high-speed capacitive humidity sensor with on-chip thermal reset, IEEE Trans. Electron. Devices 47 (2000) 702–710.
[8] M. Dokmeci, K. Najafi, A high-sensitivity polyimide capacitive relative humidity sensor for monitoring anodically bonded hermetic micropackages, J. Microelectromech. Sys. 10 (2001) 197–204.
[9] J. Laconte, V. Wilmart, D. Flandre, J. Raskin, High-sensitivity capacitive humidity sensor using 3-layer patterned polyimide sensing film, in: Proc. IEEE Sensors, Toronto, Canada, 22–24 October, 2003, pp. 372–377.
[10] E. Zampetti, S. Pantalei, A. Pecora, A. Valletta, L. Maiolo, A. Minotti, et al., Design and optimization of an ultra thin flexible capacitive humidity sensor, Sens. Actuators B 143 (2009) 302–307.
[11] C.-L. Zhao, Q.-A. Huang, M. Qin, W.-H. Li, A CMOS interdigital capacitive humidity sensor with polysilicon heaters, in: Proc. IEEE Sensors, Kona, Hawaii, 1–4 November, 2010, pp. 382–385.
[12] T. Boltshauser, C. Azeredo Leme, H. Baltes, High sensitivity CMOS humidity sensors with on-chip absolute capacitance measurement system, Sens. Actuators B 15 (1993) 75–80.
[13] C.-L. Dai, A capacitive humidity sensor integrated with micro heater and ring oscillator circuit fabricated by CMOS-MEMS technique, Sens. Actuators B 122 (2007) 375–380.
[14] C.-L. Zhao, M. Qin, Q.-A. Huang, A fully packaged CMOS interdigital capacitive humidity sensor with polysilicon heaters, IEEE Sens. J. 11 (2011) 2986–2992.
[15] N. Lazarus, G.K. Fedder, Designing a robust high-speed CMOS-MEMS capacitive humidity sensor, J. Micromech. Microeng. 22 (2012) 085021.
[16] Y. Kim, B. Jung, H. Lee, H. Kim, K. Lee, H. Park, Capacitive humidity sensor design based on anodic aluminum oxide, Sens. Actuators B 141 (2009) 441–446.
[17] M. Björkqvist, J. Salonen, J. Paski, E. Laine, Characterization of thermally carbonized porous silicon humidity sensor, Sens. Actuators A 112 (2004) 244–247.
[18] T. Wagner, S. Krotzky, A. Weiß, T. Sauerwald, C.-D. Kohl, J. Roggenbuck, et al., A high temperature capacitive humidity sensor based on mesoporous silica, Sensors 11 (2011) 3135–3144.
[19] C.-T. Wang, C.-L. Wu, I.C. Chen, Y.-H. Huang, Humidity sensors based on silica nanoparticle aerogel thin films, Sens. Actuators B 107 (2005) 402–410.
[20] C.-T. Wang, C.-L. Wu, Electrical sensing properties of silica aerogel thin films to humidity, Thin Solid Films 496 (2006) 658–664.
[21] V.P.J. Chung, J.K.-C. Liang, C.-L. Cheng, M.-C. Yip, W. Fang, Development of a CMOS-MEMS RF-aerogel-based capacitive humidity sensor, in: Proc. IEEE Sensors, Valencia, Spain, 2014, pp. 190–193.
[22] L.M. Hair, R.W. Pekala, R.E. Stone, C. Chen, S.R. Buckley, Low-density resorcinol–formaldehyde aerogels for direct-drive laser inertial confinement fusion targets, J. Vacuum Sci. Technol. A 6 (1988) 2559–2563.
[23] R.W. Pekala, Organic aerogels from the polycondensation of resorcinol with formaldehyde, J. Mater. Sci. 24 (1989) 3221–3227.
[24] M.-H. Tsai, C.-M. Sun, Y.-C. Liu, C. Wang, W. Fang, Design and application of a metal wet-etching post-process for the improvement of CMOS-MEMS capacitive sensors, J. Micromech. Microeng. 19 (2009) 105017.
[25] Silicon Laboratories Inc. Si7007-A10 datasheet; 2014.
[26] Z.-S. Feng, X.-J. Chen, J.-J. Chen, J. Hu, A novel humidity sensor based on alumina nanowire films, J. Phys. D: Appl. Phys. 45 (2012) 225305.

Biographies

Vincent P. J. Chung was born in Connecticut, USA. He received the B.S. and M.S. degrees from the Power Mechanical Engineering in National Tsing Hua University, Taiwan, in 2012 and in 2014, respectively. His research interests include RF MEMS, CMOS–MEMS technology and integrated circuit design.

Ming-Chuen Yip is an expert on the experimental mechanics of nanocomposite materials, with more than 10 years of experience in teaching and research in this area. His research interests include fatigue, creep and fracture properties of nanocomposite materials. He was the chairman of the Society of Theoretical and Applied Mechanics in Taiwan, and was also the president of the Asian Australasian Association for Composite Materials.

Weileun Fang was born in Taipei, Taiwan. He received his Ph.D. degree from Carnegie Mellon University in 1995. His doctoral research focused on the determining of the mechanical properties of thin films using micromachined structures. In 1995, he worked as a postdoctoral research at Synchrotron Radiation Research Center, Taiwan. He joined the Power Mechanical Engineering Department at the National Tsing Hua University (Taiwan) in 1996, where he is now a Distinguished Professor as well as a faculty of NEMS Institute. In 1999, he was with Prof. Y.-C. Tai at California Inst. Tech. as a visiting associate. His research interests include MEMS with emphasis on micro fabrication/packaging technologies, CMOS MEMS, CNT MEMS, micro optical systems, micro sensors and actuators, and characterization of thin film mechanical properties. Prof. Fang has published more than 140 SCI journal papers, near 250 international conference papers, and 80 patents (all in MEMS field). He is now the Editor-in-Chief of JMM, the Board Member of IEEE TDMR, and the Associate Editor of IEEE Sensors J., and Sensors and Actuators A. He served as the chief delegate of Taiwan for World Micromachine Summit (MMS) from 2008–2012, and chaired the MMS 2012. He also served as the TPC of IEEE MEMS conference, the EPC of Transducers conference, and the regional co-chair as well as TPC chair of IEEE Sensors conference. He has become the member of international steering committee of Transducers from 2009. Moreover, he also serves as a technical consultant for many MEMS companies in Taiwan.